

## **Genotype-Adaptive Regulatory Mechanisms of Nano-Silicon in Alleviating Cadmium Toxicity in Pakchoi**

Kan Huang<sup>1</sup>, Zongfeng Hu<sup>1</sup>, Songwei Wu<sup>1</sup>, Qiling Tan<sup>1</sup>, Chengxiao Hu<sup>1</sup>, Xuecheng Sun<sup>1, 2, 3\*</sup>

<sup>1</sup>Key Laboratory of Arable Land Conservation (Middle and Lower Reaches of Yangtze River), Ministry of Agriculture, Micro-elements Research Center, College of Resources & Environment, Huazhong Agricultural University, Wuhan, 430070, China

<sup>2</sup>Shenzhen Institute of Nutrition and Health, Huazhong Agricultural University, Wuhan, 430070, China

<sup>3</sup>Shenzhen Branch, Guangdong Laboratory for Lingnan Modern Agriculture, Genome Analysis Laboratory of the Ministry of Agriculture, Agricultural Genomics Institute at Shenzhen, Chinese Academy of Agricultural Sciences, Shenzhen, 518000, China

Correspondence: Xuecheng Sun ([sxccn@mail.hzau.edu.cn](mailto:sxccn@mail.hzau.edu.cn))

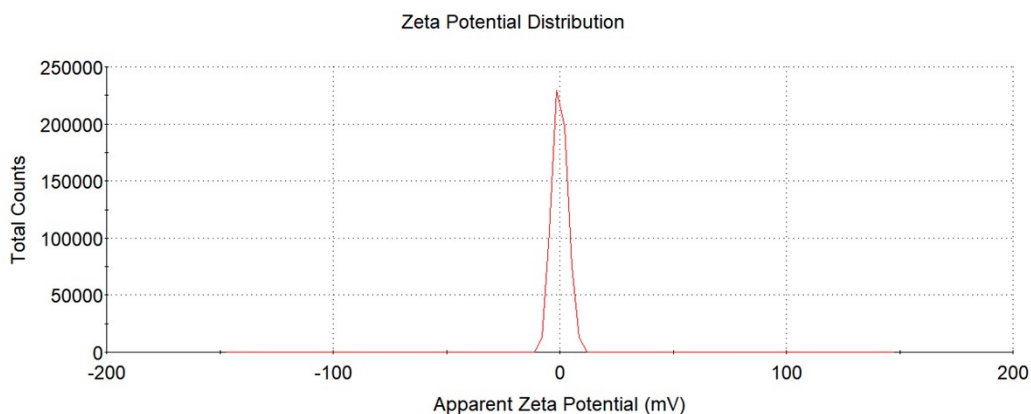


Figure S1. The synthesized SiO<sub>2</sub> nanoparticles exhibit a narrow and near-neutral  $\zeta$ -potential distribution, indicating good colloidal stability in ethanol. This figure presents the apparent  $\zeta$ -potential distribution (in mV) of the SiO<sub>2</sub> nanoparticle sample. The x-axis represents apparent  $\zeta$ -potential (range: -200 to +200 mV), and the y-axis shows total counts detected. A single sharp peak is observed near 0 to -5 mV, suggesting uniform surface charge distribution and low aggregation, with no additional or multimodal peaks present.  $\zeta$ -potential was measured using dynamic light scattering (DLS) in electrophoretic mobility mode under standard aqueous conditions (25 °C). Each sample was analyzed with three technical replicates (N = 3), and the curve represents the averaged distribution; no error bars are shown, as the instrument outputs probability distribution curves rather than discrete values.

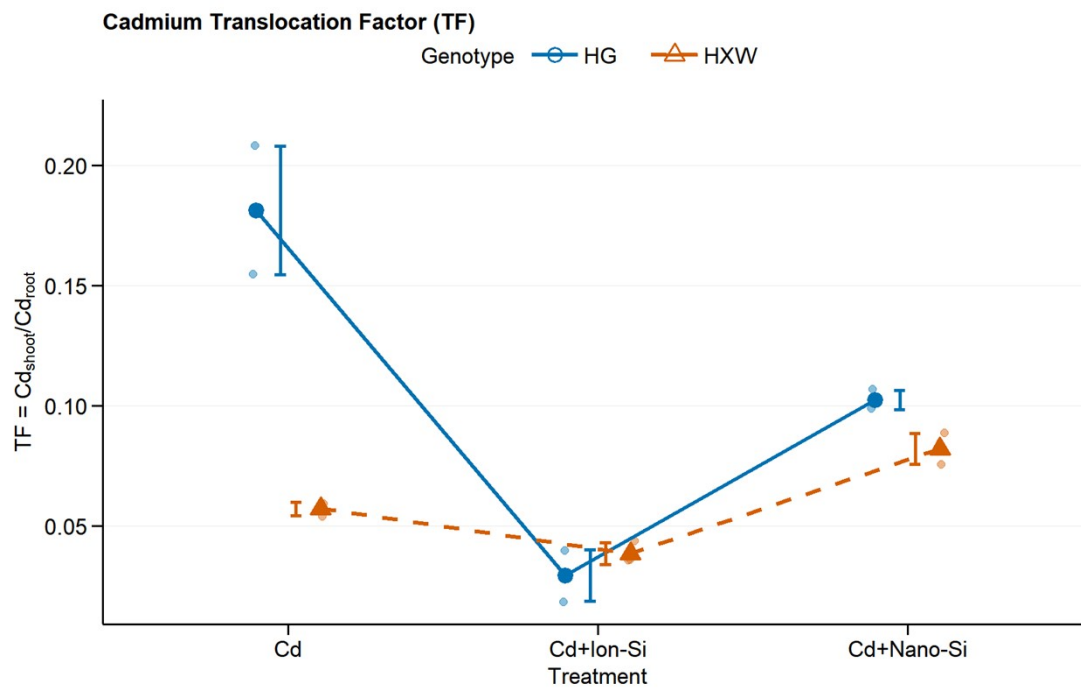


Figure S2. Silicon application reduced the Cd translocation factor (TF) from root to shoot in both genotypes, with Nano-Si exhibiting the most pronounced inhibitory effect. The line chart shows Cd translocation factor (TF =  $Cd_{shoot}/Cd_{root}$ ) for genotypes HG (blue open circles, solid line) and HXW (orange open triangles, dashed line) under three treatments: Cd, Cd+Ion-Si, and Cd+Nano-Si. The y-axis represents TF values; each data point is the mean of three biological replicates (N = 3), with vertical error bars indicating standard deviation (SD).

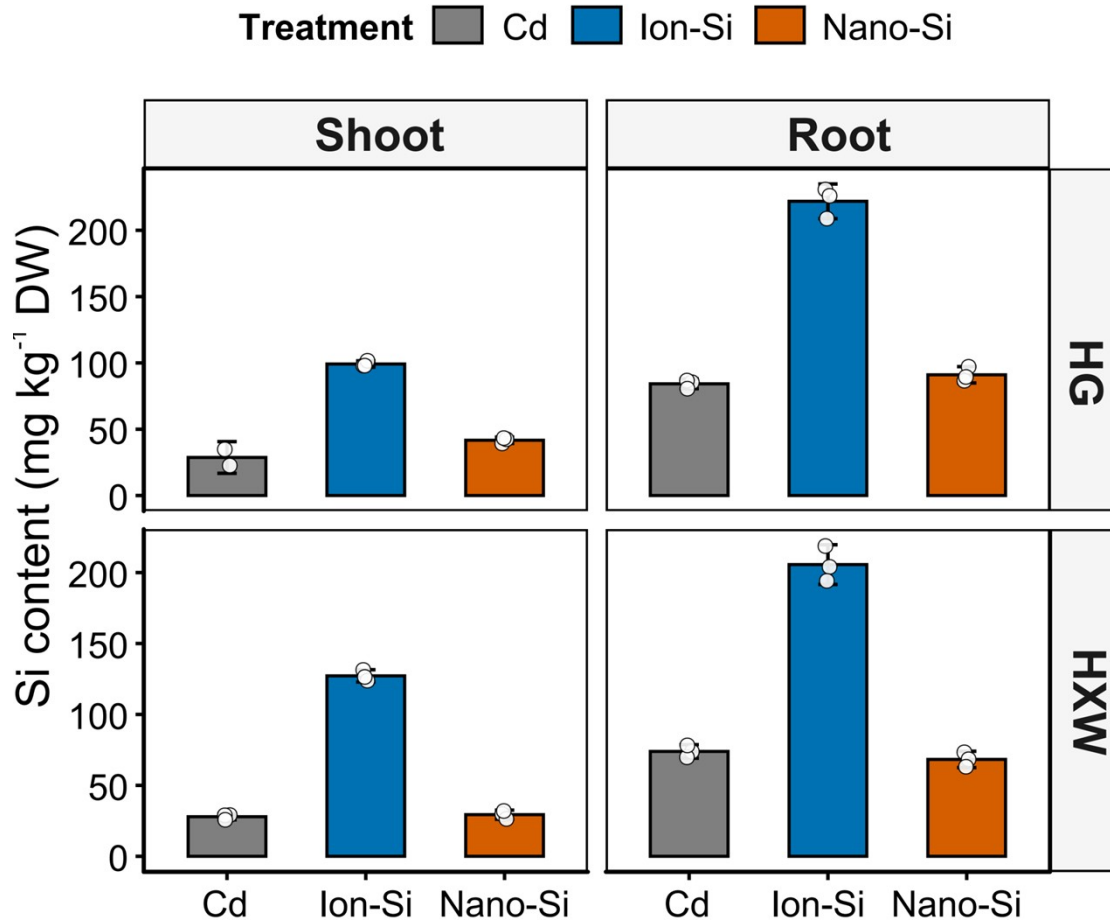


Figure S3. Both Ion-Si and Nano-Si treatments significantly increased Si content in plants, particularly in roots, with HG exhibiting the highest Si uptake under Ion-Si. The bar chart shows Si content (mg kg<sup>-1</sup> dry weight) in shoots and roots of genotypes HG and HXW under three treatments: Cd (control, gray), Ion-Si (blue), and Nano-Si (orange). Each bar represents the mean of three biological replicates (N = 3), with vertical error bars indicating standard deviation (SD) and white dots atop bars denoting individual replicate values. Subplot layout: top row for HG (left: shoot; right: root), bottom row for HXW (left: shoot; right: root). Within each genotype × tissue combination, one-way ANOVA was performed followed by Tukey's post-hoc test; significant differences were determined at  $p < 0.05$ .

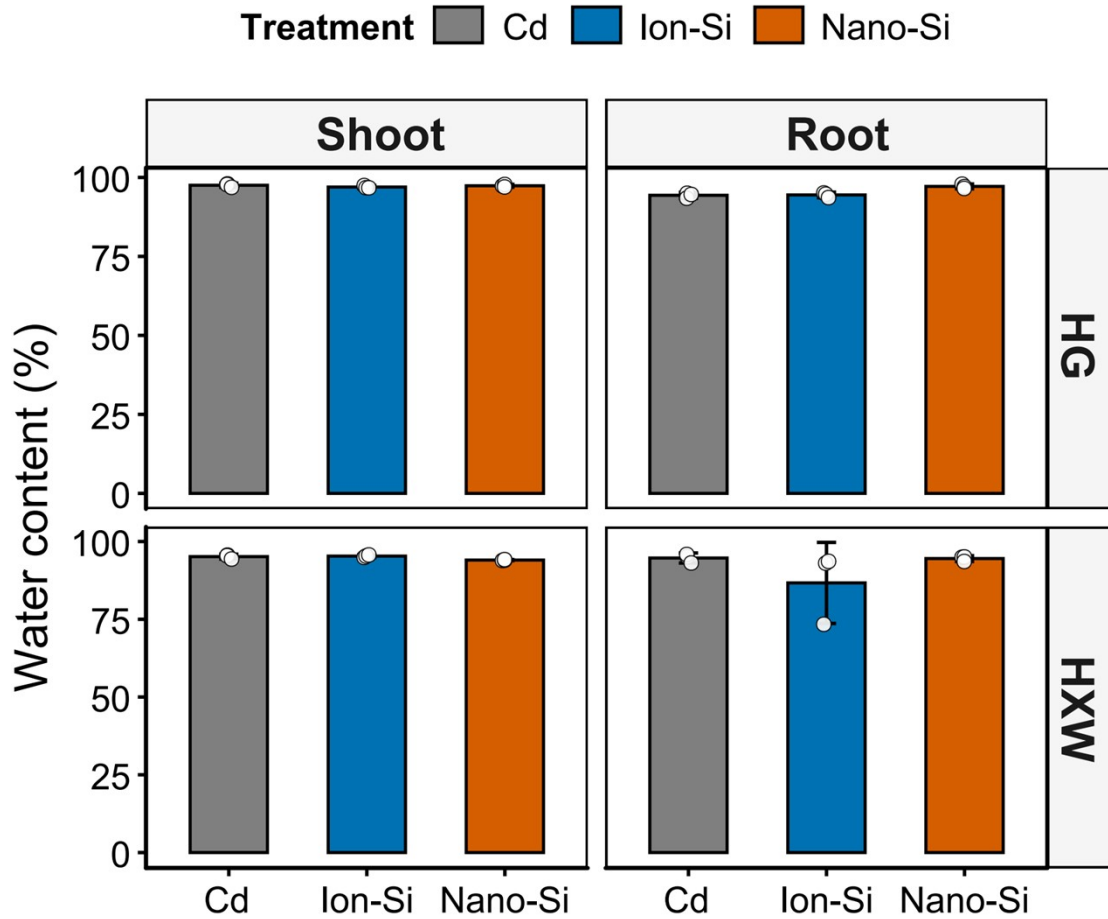


Figure S4. Silicon application exerted minimal effects on tissue water content, with only a slight decrease observed in HXW roots under Ion-Si treatment. The bar chart shows water content (%) in shoots and roots of genotypes HG and HXW under CK (gray), Ion-Si (blue), and Nano-Si (orange) treatments. Subplots are arranged by genotype and tissue: top row for HG, bottom row for HXW; left column for shoots, right column for roots. Each bar represents the mean of three biological replicates ( $N = 3$ ), with error bars indicating standard deviation (SD) and white dots atop bars denoting individual replicate values. Within each genotype–tissue combination, one-way ANOVA followed by Tukey’s multiple comparison test was performed. No significant differences ( $p < 0.05$ ) were detected except where specifically indicated in the raw data.

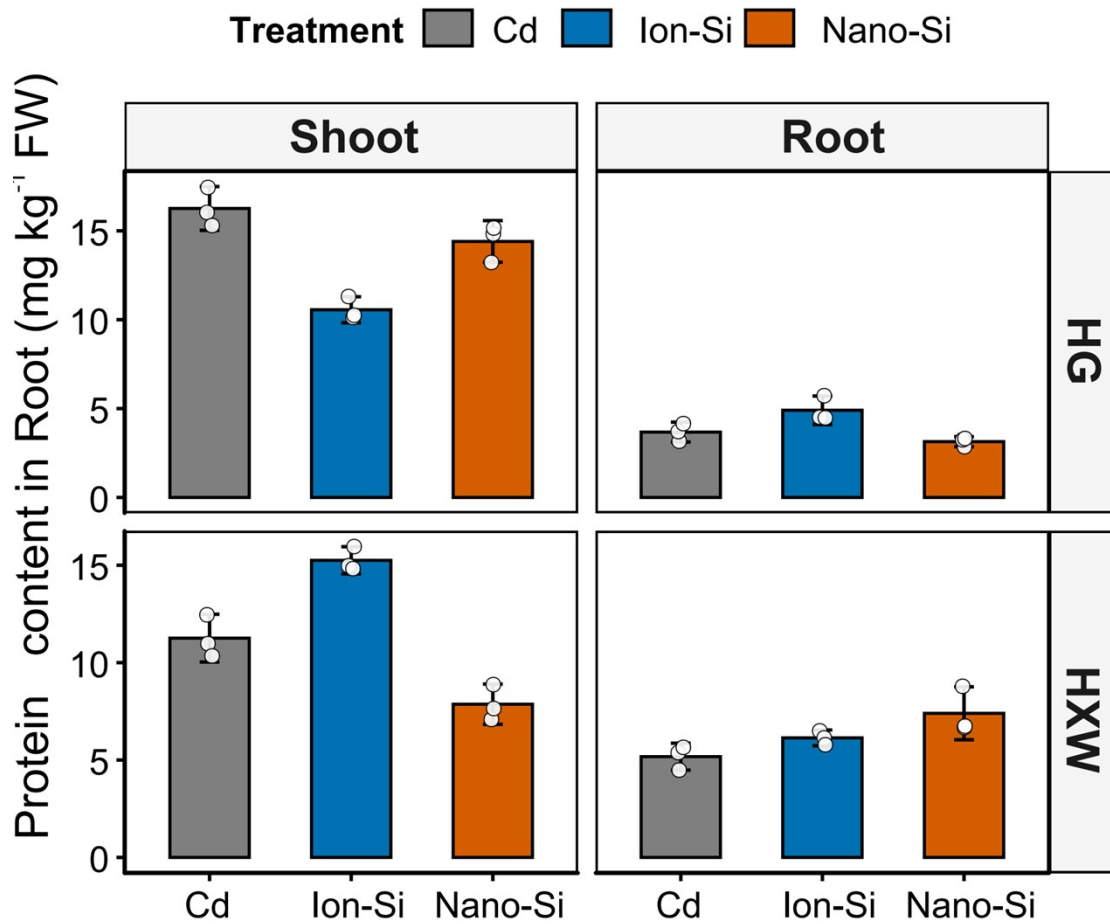


Figure S5. Protein content varied across genotypes and treatments, with Ion-Si treatment generally increasing protein levels, most notably in HXW shoots. The bar chart shows protein content (mg kg<sup>-1</sup> fresh weight) in shoots and roots of genotypes HG and HXW under CK (gray), Ion-Si (blue), and Nano-Si (orange) treatments. White dots atop bars represent individual biological replicate values, error bars indicate standard deviation (SD), and each bar is the mean of three biological replicates (N = 3). Subplots are arranged by genotype (top: HG; bottom: HXW) and tissue (left: shoot; right: root). Statistical analysis was performed using one-way ANOVA followed by Tukey's post-hoc test, with significance at  $p < 0.05$ .